journal homepage: www.intl.elsevierhealth.com/journals/cmpb

Computer-aided diagnosis of breast masses using quantified BI-RADS findings

Woo Kyung Moon[a,1], Chung-Ming Lo[b,1], Nariya Cho[a], Jung Min Chang[a], Chiun-Sheng Huang[c], Jeon-Hor Chen[d,e], Ruey-Feng Chang[b,f,*]

[a] Department of Radiology, Seoul National University Hospital, Seoul, Republic of Korea
[b] Department of Computer Science and Information Engineering, National Taiwan University, Taipei, Taiwan
[c] Department of Surgery, National Taiwan University Hospital and National Taiwan University College of Medicine, Taipei, Taiwan
[d] Center for Functional Onco-Imaging, Department of Radiological Science, University of California, Irvine, CA, USA
[e] Department of Radiology, E-Da Hospital and I-Shou University, Kaohsiung, Taiwan
[f] Graduate Institute of Biomedical Electronics and Bioinformatics, National Taiwan University, Taipei, Taiwan

ARTICLE INFO

Article history:
Received 20 October 2012
Received in revised form
20 February 2013
Accepted 31 March 2013

Keywords:
Breast cancer
Ultrasound
Computer-assisted diagnosis
Breast Imaging Reporting and Data System

ABSTRACT

The information from radiologists was utilized in the proposed computer-aided diagnosis (CAD) for breast tumor classification. The ultrasound (US) database used in this study contained 166 benign and 78 malignant masses. For each mass, six quantitative feature sets were used to describe the radiologists' grading of six Breast Imaging Reporting and Data System (BI-RADS) categories including shape, orientation, margins, lesion boundary, echo pattern, and posterior acoustic features on breast US. The descriptive abilities were between 76% and 82% and the predicted descriptors were then used for tumor classification. Using receiver operating characteristic curve for evaluation, the area under curve (AUC) of the proposed CAD was slightly better than that of a conventional CAD based on the combination of all quantitative features (0.96 vs. 0.93, $p = 0.18$). The partial AUC over 90% sensitivity of the proposed CAD was significantly better than that of the conventional CAD (0.90 vs. 0.76, $p < 0.05$). In conclusion, the computer-aided analysis with qualitative information from radiologists showed a promising result for breast tumor classification.

1. Introduction

Breast ultrasound (US) is commonly used to distinguish benign from malignant masses. The Breast Imaging Reporting and Data System (BI-RADS) lexicon was developed by the American College of Radiology [1] to standardize the terminology and assessment of clinical examination. For radiologists to evaluate lesions, the dominant sonographic characteristics are described according to six BI-RADS descriptive categories: shape, orientation, margins, lesion boundary, echo pattern, and posterior acoustic features. The BI-RADS lexicon was confirmed so that radiologists can obtain good agreement when analyzing US images to classify masses [2]. To provide more efficient procedure for diagnosis, various computer-aided diagnosis (CAD) systems have been developed to quantize the tumor characteristics used by radiologists [3,4]. Based on the segmentation of tumor area, morphology features were proposed to describe tumor shape and texture features were suggested to describe tumor echogenicity. According

* *Corresponding author at*: Department of Computer Science and Information Engineering, National Taiwan University, Taipei 10617, Taiwan, ROC. Tel.: +886 2 33661503; fax: +886 2 23628167.
E-mail address: rfchang@csie.ntu.edu.tw (R.-F. Chang).

[1] These authors are co-first authors based on equal contributions in separate (medicine and engineering) components of the study.

0169-2607/$ – see front matter © 2013 Elsevier Ireland Ltd. All rights reserved.
http://dx.doi.org/10.1016/j.cmpb.2013.03.017

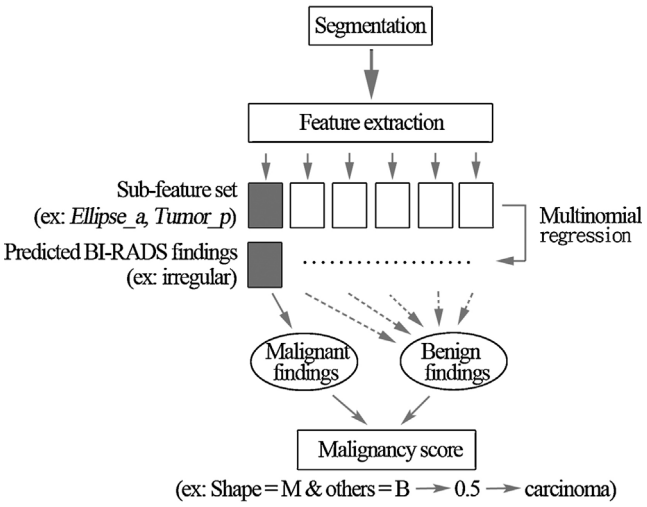

Fig. 1 – The organization of the proposed CAD system. Six quantified BI-RADS findings were used to determine the malignancy score. In our CAD algorithm, any tumor with one or more malignant findings was classified as malignant. Only the tumors that had no malignant findings and had at least one benign finding were classified as benign.

to the biopsy-proven result, the quantitative features were simply combined to classify tumors into benign or malignant in the CAD systems. However, the quantitative features were developed without radiologists' confirmations. Whether the quantitative features have successfully interpreted the malignancy of tumors is uncertain in the conventional CAD systems.

In this study, the sonographic interpretation of six BI-RADS descriptive categories from expert breast radiologists were quantified using six relevant feature sets for tumor classification. In our CAD algorithm, any tumor with one or more malignant findings was classified as malignant. Only the tumors that had no malignant findings and had at least one benign finding were classified as benign. The organization of the proposed CAD system is shown in Fig. 1. The performance of the proposed CAD system was compared to that from a conventional CAD system using only quantitative features.

2. Materials and methods

2.1. Patients and data acquisition

This study was approved by our institution review board, and informed consent was waived for this retrospective study. From January 2003 to July 2004, a total of 244 patients with suspicious findings on US images underwent core needle biopsy or fine-needle aspiration cytology. These US images were acquired using an ATL HDI 5000 scanner (Philips, Bothell, WA) with linear probe with a frequency of 5–12 MHz. The biopsy-proven tumors used in this study included 166 (68%) benign and 78 (32%) malignant tumors. The benign tumors included 103 cases of fibroadenoma and 63 cases of fibrocystic changes. The malignant tumors included 76 cases of invasive ductal carcinoma and 2 cases of invasive papillary carcinoma. The mean age of patients with benign tumors was 44 (range 21–65), and the patients with malignant tumors had a mean age of 49 (range 33–70).

Two breast radiologists who were blinded to the pathologic report classified the tumors of all patients into BI-RADS assessment categories according to the US findings in consensus [2]. The radiologists had 5 and 15 years of experience with breast US. There were 52 (21%) tumors in BI-RADS 3 (probably benign), 148 (61%) tumors in BI-RADS 4 (suspicious abnormality), and 44 (18%) tumors in BI-RADS 5 (highly suggestive of malignancy). The sonographic characteristics of the tumors including shape, orientation, margins, lesion boundary, echo pattern, and posterior acoustic features are summarized in Table 1.

2.2. Tumor segmentation

To quantify the tumor characteristics, the tumors had to be segmented first. The level set method [5] was employed as a segmentation tool to separate the tumors from background tissues. In the beginning, the image contrast was improved using a sigmoid filter [6]. Fig. 2(b) shows the result of applying the sigmoid filter in Fig. 2(a), the original sonographic image. Next, the gradient image, which presents the intensity variations in the horizontal and vertical directions, was calculated with the gradient magnitude filter [7] on the contrast-enhanced image. Fig. 2(c) shows the gradient magnitude image of Fig. 2(b). Then, the sigmoid filter was applied again to the gradient magnitude image for contrast enhancement, as shown in Fig. 2(d). After preprocessing, the level set method, proposed to model a complex shape with changing topology, was applied to the enhanced gradient image for outlining the contour of tumors. Fig. 2(e) shows the result of applying the level set method in Fig. 2(d).

2.3. Quantitative features

The quantitative features extracted from the segmented tumors can be classified into two groups: morphology and texture features. Morphological features were used to describe the geometric characteristics of the tumors, such as shape, orientation, and margins. To extract the morphological features, the best-fit ellipse was utilized for approximating the size and position of each tumor. For example, the tumor orientation can be computed by the angle of the major axis of the ellipse. Other studies developed quantitative features based directly on the original properties of tumors. Rangayyan et al. [8] estimated the compactness of tumors according to the perimeter and area. Nie et al. [9] proposed the use of the normalized radial length (NRL) to describe the roundness of tumors. The NRL was defined as the Euclidean distance between the tumor center and the pixels on the tumor boundary normalized by the maximum distance.

The other group of quantitative features is texture features. Texture features were used to describe the tissue composition inside the tumor [9]. Different tissues have different echogenicity patterns that result in various distributions of gray level values. Gray level co-occurrence matrices (GLCM)

Table 1 – The sonographic characteristics of 244 breast masses graded by the radiologists.

Category	Descriptors	Malignant ($n = 78$)	Benign ($n = 166$)	Total number ($n = 244$)
Shape	Round	0	0	0
	Oval	1	99	100
	Irregular	77	67	144
Orientation	Parallel	54	148	202
	Not parallel	24	18	42
Margin	Circumscribed	1	46	47
	Not circumscribed			
	Microlobulated	2	95	97
	Indistinct	0	0	0
	Angular	37	25	62
	Spiculated	38	0	38
Lesion boundary	Abrupt interface	36	162	198
	Echogenic halo	42	4	46
Echo pattern	Hyperechoic	0	9	9
	Isoechoic	1	93	94
	Hypoechoic	77	64	141
	Complex	0	0	0
	Anechoic	0	0	0
Posterior acoustic features	Enhancement	12	24	36
	No posterior acoustic feature	45	140	185
	Shadowing	10	2	12
	Combined pattern	11	0	11

provide the statistical information to determine the spatial correlations between pixels inside a region [10]. To extend the comparison between two regions, the average intensity of a region can be subtracted from that of another region to show the dissimilarity. Therefore, the transitions between the tumor and the surrounding tissues, such as echo halo and posterior shadowing, can be expressed by the average intensity difference [11]. In Table 2, a total of 38 quantitative features mentioned above were collected to predict the radiologists' grading in six BI-RADS descriptive categories (Table 1). The corresponding quantified tumor characteristics are shown in Fig. 3.

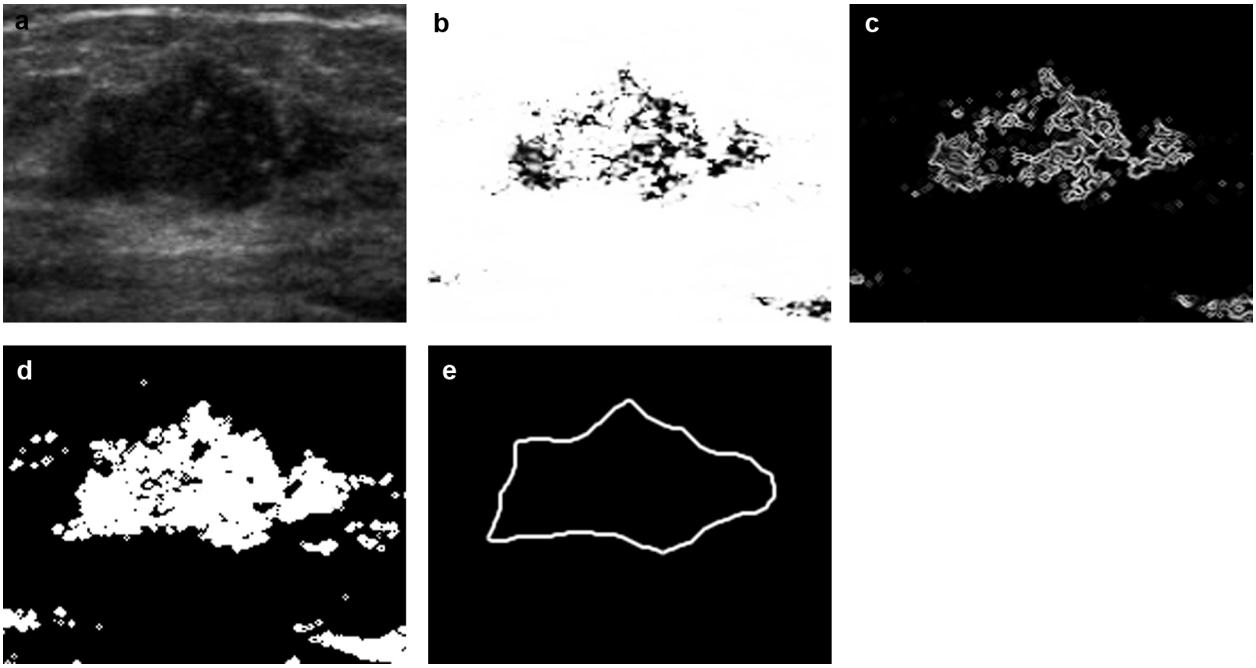

Fig. 2 – Illustration of the segmentation procedure with the preprocessing steps: (a) The original sonographic image; (b) after applying the sigmoid filter to the original image; (c) after applying the gradient magnitude filter to (b); (d) after applying the sigmoid filter to (c); and (e) the contour segmented by the level set method.

Table 2 – 38 quantitative features.

Category	Feature	Description
Morphology	*Tumor_a*, *Tumor_p*	Tumor area and perimeter
	Ellipse_a, *Ellipse_b*, *Ellipse_a/b*, *Ep/Tp*, *Ellipse_compactness*, *Ellipse_theta*	Best-fit ellipse features *Ellipse_a*: the length of the major axis *Ellipse_b*: the length of the minor axis *Ellipse_a/b*: *Ellipse_a/Ellipse_b* *Ep/Tp*: the ratio of the ellipse perimeter and the tumor perimeter *Ellipse_compactness*: the overlap between the ellipse and the tumor *Ellipse_theta*: the angle of the major axis of the ellipse [13]
	NRL entropy, *NRL variance*	NRL features [9]
	Compactness	Tumor roundness [8]
	Undulation, *Sharp*, *MU*	Features about undulations on the tumor boundary [11]
	NS, *MNS*, *MaxSpicule*	*NS*: the number of spicules on the tumor boundary *MNS*: modified *NS* *MaxSpicule*: the length of the longest spicule of *NS*
Texture	*LB*	The average intensity difference between the inner and outer bands around the tumor boundary [11]
	PS, *PS_diff*	*PS*: the average intensity difference between the tumor and the region under the tumor [11] *PS_diff*: the average intensity difference between the surrounding tissues and the region under the tumor
	EPc, *EP_diff*	*EPc*: the average intensity difference between the 25% brighter pixels and whole tumor pixels [11] *EP_diff*: the average intensity difference between the tumor and the surrounding tissues
	Energy ave., *Energy std.*, *Entropy ave.*, *Entropy std.*, *Correlation ave.*, *Correlation std.*, *Inverse Difference Moment ave.*, *Inverse Difference Moment std.*, *Inertia ave.*, *Inertia std.*, *Cluster Shade ave. Cluster Shade std.*, *Cluster Prominence ave.*, *Cluster Prominence std.*, *Haralick Correlation ave.*, *Haralick Correlation std.*	16 GLCM features [10]

2.4. *Classification*

Taking the grading of the radiologists as the ground truth, the implemented quantitative features were used to predict the descriptors in each category with the multinomial regression model [12]. According to the suggestions in previous studies for quantifying tumor characteristics [8,9,11,13], one or more quantitative features were selected manually to predict the individual BI-RADS descriptive categories. For example, 16 GLCM features were used to predict the echo pattern of each tumor to be hypoechoic, hyperechoic, or isoechoic. In the classifier of multinomial regression model, the features were examined to generate the best combining performance. Backward elimination was applied in the stepwise procedure for feature selection. While the least error rate was obtained from the trained classifier, the corresponding subset of features was selected to be the most relevant to the category. The performance of the classifier was examined by the leave-one-out cross validation method [14].

After selection, the six BI-RADS descriptive categories of each tumor can be predicted using the selected features. These predicted BI-RADS findings were regarded as malignant or benign findings according to Table 3 which was constructed by means of the BI-RADS descriptors' appearance frequencies in benign and malignant tumors as shown in Table 1. With the Mann–Whitney *U* test [15], each descriptor was tested if it is significant in differentiating malignant tumors from benign tumors. Upon the radiologists' assessment, we used 1 for existence and 0 for nonexistence to generate numerical data for statistical analysis. The result in Table 3 shows that the evaluated malignant or benign findings in each descriptive category all had a p-value less than 0.05. That is, these malignant or benign findings were all significant in distinguishing malignant tumors from benign tumors. At the end, the diagnostic algorithm used a decision tree to classify tumors. Any tumor with one or more malignant findings was classified as malignant. Only the tumors that had no malignant findings and at least one benign finding were classified as benign.

2.5. *Statistical analysis*

In the classification result, the performance was evaluated based on five indices: accuracy, sensitivity, specificity, positive predictive value (PPV), and negative predictive value (NPV) based on the biopsy-proven pathology. With the Chi-square test, the performance indices of a conventional CAD method, which combined all quantitative features together in the multinomial regression model for diagnosis, were compared to those of the proposed method. The performance of the classifier was also examined by the leave-one-out cross validation method. With X cases involved in the cross validation, these X cases were trained X times. Each time, one separate case was left out of the X cases and was used to test the result trained by the rest cases. Besides, the trade-offs between sensitivity

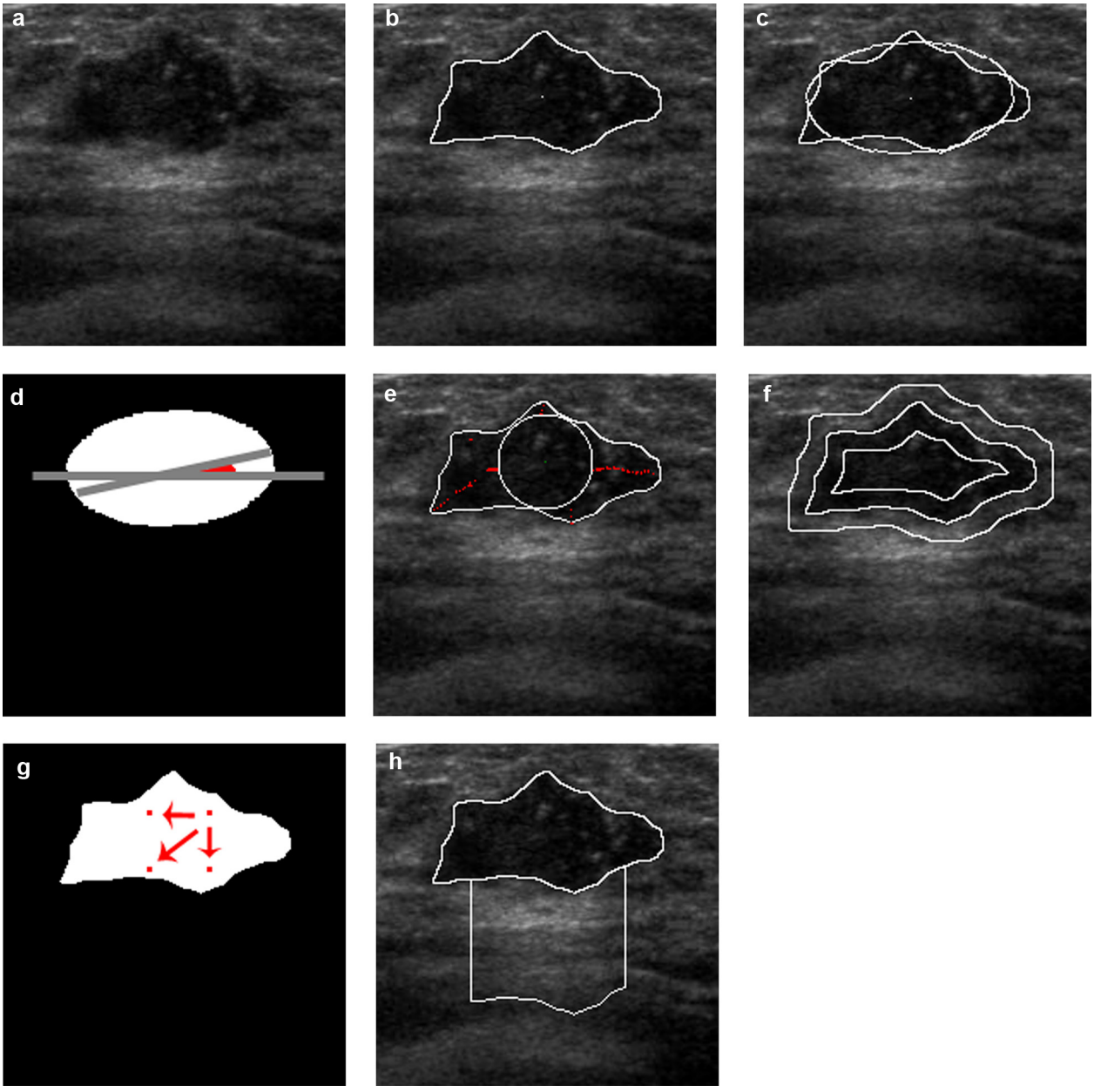

Fig. 3 – The illustration of the quantification for tumor characteristics based on six BI-RADS descriptive categories: (a) the original US image of a tumor; (b) the segmentation result of (a); (c) the length of the major axis of the best-fit ellipse was compared to tumor perimeter for the quantification of shape (*Ellipse_a* = 61, *Tumor_p* = 419); (d) the angle between the major axis of the ellipse and the horizontal line was used for the quantification of orientation (*Ellipse_theta* = 15); (e) the undulations on tumor boundary was used for the margin quantification (*NRL entropy* = 2.7); (f) the average intensity difference between the inner and outer bands around the tumor boundary was used for boundary quantification (*LB* = 38); (g) GLCM features used for determining the spatial correlations between pixels inside a tumor were quantified for echo pattern (*Correlation std* = 0.03); and (h) the average intensity difference between the tumor and the region under the tumor was used to quantify posterior acoustic features (*PS* = 50).

and specificity in the two CAD systems were compared using the receiver operating characteristic (ROC) curve. To determine the malignancy score of each tumor, the rule of the diagnostic algorithm was followed. That is, a tumor with one malignant finding was given a score of 0.5. One more malignant finding increases 0.1 of the score. Tumors with 2–6 malignant findings were given a score from 0.6 to 1. Tumors with no malignant findings were regarded as benign and were given a score of 0. By this way, a complete ROC curve with continuous operating points can be generated. The normalized area under the curve (AUC) and the partial area under the curve (pAUC) above 90% sensitivity were measured for comparison via the bootstrap method implemented in the pROC package [16]. The test methods used in this study were all performed

Table 3 – Malignant and benign descriptors chosen by the radiologists.

Category	Malignant	Benign	*p*-Value
Shape	Irregular	Oval	<0.001*
Orientation	Not parallel	Parallel	<0.001*
Margin	Angular, spiculated	Circumscribed, microlobulated	<0.001*
Lesion boundary	Echogenic halo	Abrupt interface	<0.001*
Echo pattern	Hypoechoic	Hyperechoic, isoechoic	<0.001*
Posterior acoustic features	Shadowing, combined pattern	Enhancement, no posterior acoustic feature	<0.001*

* *p*-Value <0.05 shows the statistically significant difference.

with SPSS software (version 16 for Windows; SPSS, Chicago, IL, USA).

3. Results

Table 4 shows the selected quantitative features and their performances. The performances of features related to orientation and lesion boundary were the most accurate (82%), whereas the performance of features related to echo pattern was the least accurate (76%). However, the difference was not statistically significant ($p > 0.05$). Fig. 3 shows the quantification of tumor characteristics based on six BI-RADS descriptive categories.

For comparison, the conventional CAD system employed 32 features from all features after feature selection. The eliminated features were *Ellipse_a*, *Ep/Tp*, *Undulation*, *NRL entropy*, *Ellipse_compactness*, and *PS*. The differences of AUC and pAUC over 90% sensitivity in the two CAD systems are shown in Fig. 4. The AUC and pAUC of the proposed CAD system were 0.96 and 0.90, respectively. The AUC and pAUC of the conventional CAD system were 0.93 and 0.76, respectively. The difference in the AUC was not statistically significant ($p = 0.18$), however the pAUC difference above 90% sensitivity was statistically significant ($p < 0.05$).

For more detailed information, the specificity comparisons at different cut-off points of high sensitivity are listed in Table 5. With the Chi-square test, the specificities of the proposed CAD system were all significantly ($p < 0.05$) higher than those of the conventional CAD system in the sensitivity range from 90% to 100%.

Fig. 5 shows an example of a malignant tumor classified correctly by both the proposed CAD algorithm and the conventional CAD method and Fig. 6 shows an example of a malignant tumor classified correctly by the proposed CAD algorithm but misclassified by the conventional CAD method.

4. Discussion

In previous studies, breast US CAD systems employed all quantitative features together to distinguish malignant tumors from benign tumors. However, it is a challenge for the classification method used in previous CAD systems to deal with the high heterogeneity of malignant tumors. Circumscribed cancers such as mucinous or medullary histologies and high-grade tumors often do not have characteristic malignant findings on US [17,18] and can be misclassified as benign by the conventional US CAD system. In this study, ACR BI-RADS and Stavros' diagnostic algorithm were implemented in the CAD system [19,20]. The main purpose of this algorithm was to classify tumors with suspicious abnormalities as malignant for high sensitivity. Considering the trade-offs between sensitivity and specificity, the proposed CAD system outperformed the conventional CAD system significantly with respect to the pAUC above 90% sensitivity (0.90 vs. 0.76, $p < 0.05$). Our result shows that the proposed CAD system using the diagnostic algorithm have the potential to prevent biopsy of benign tumors without missing malignant tumors, and the proposed system is expected to be more appropriate for clinical diagnosis than conventional CAD systems.

CAD models using radiologist-interpreted mammographic or sonographic descriptors have been published previously [21,22]. These authors used radiologist-interpreted features as one of the input features for CAD models to differentiate benign from malignant tumors. In contrast, we used features extracted directly from US images in this study. The rule of the diagnostic algorithm used in our CAD system is similar to the

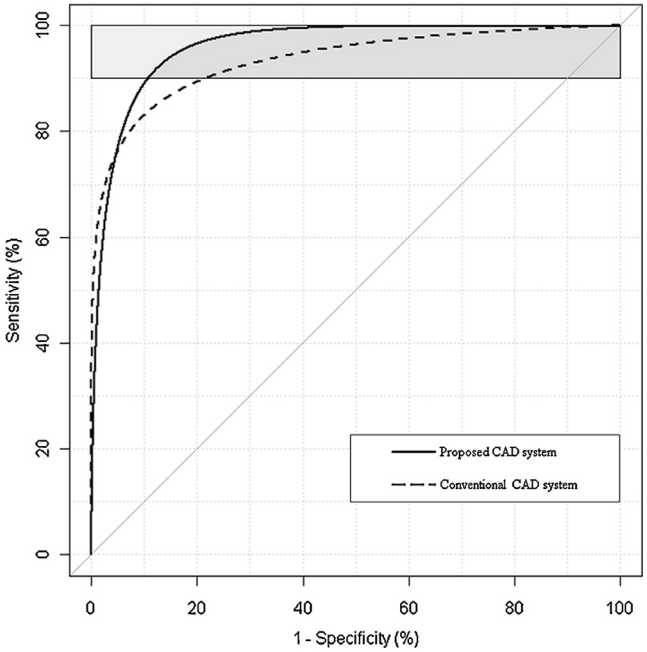

Fig. 4 – The ROC curves of the proposed CAD system (the solid line) and the conventional CAD system (the dashed line). The AUC and pAUC of the proposed CAD system were 0.96 and 0.90, respectively. The AUC and pAUC of the conventional CAD system were 0.93 and 0.76, respectively. The difference in the AUC was not statistically significant ($p = 0.18$), while the pAUC difference above 90% sensitivity was statistically significant ($p < 0.05$).

Table 4 – The selected features for each descriptive category and the performance of these factors.

Category	Features	Accuracy (%)
Shape	*Ellipse_a*, *Tumor_p*	80
Orientation	*Ellipse_theta*	82
Margin	*Compactness*, *NRL entropy*, *Ep/Tp*, *Ellipse_a/b*, *EP_diff*, *MNS*	77
Lesion boundary	*LB*	82
Echo pattern	*Correlation std*, *Inverse Difference Moment ave*, *Cluster Shade ave*, *Cluster Prominence ave*, *Haralick Correlation ave*, *Haralick Correlation std*	76
Posterior acoustic features	*PS*	78

Table 5 – The specificity comparison between the proposed CAD system and the conventional system above 90% sensitivity.

Sensitivity	Performance indices	Proposed CAD system	Conventional CAD system	*p*-Value
90%	Specificity	89% (148/166)	79% (131/166)	0.01*
	Accuracy	89% (218/244)	82% (201/244)	
	PPV	80% (70/88)	67% (70/105)	
	NPV	95% (148/156)	94% (131/139)	
95%	Specificity	84% (139/166)	60% (100/166)	<0.001*
	Accuracy	87% (213/244)	71% (174/244)	
	PPV	73% (74/101)	53% (74/140)	
	NPV	97% (139/143)	96% (100/104)	
97%	Specificity	79% (131/166)	46% (76/166)	<0.001*
	Accuracy	85% (207/244)	62% (152/244)	
	PPV	68% (76/111)	46% (76/166)	
	NPV	98% (131/133)	97% (76/78)	
99%	Specificity	68% (113/166)	22% (37/166)	<0.001*
	Accuracy	78% (190/244)	47% (114/244)	
	PPV	59% (77/130)	37% (77/206)	
	NPV	99% (113/114)	97% (37/38)	
100%	Specificity	37% (61/166)	4% (7/166)	<0.001*
	Accuracy	57% (139/244)	35% (85/244)	
	PPV	43% (78/183)	33% (78/237)	
	NPV	100% (61/61)	100% (7/7)	

* *p*-Value < 0.05 shows the statistically significant difference.

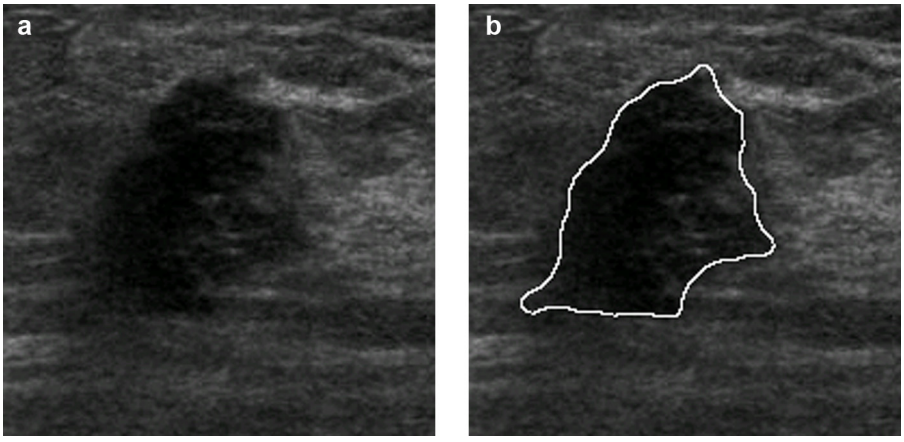

Fig. 5 – An example of a malignant tumor classified correctly by both the proposed CAD algorithm and the conventional CAD method. Among six predicted BI-RADS findings of this tumor, there were four malignant findings: irregular, not parallel, spiculated, and hypoechoic. The malignancy score of this tumor is 0.8 in the diagnostic algorithm. (a) The original sonographic image and (b) The contour was outlined for feature extraction.

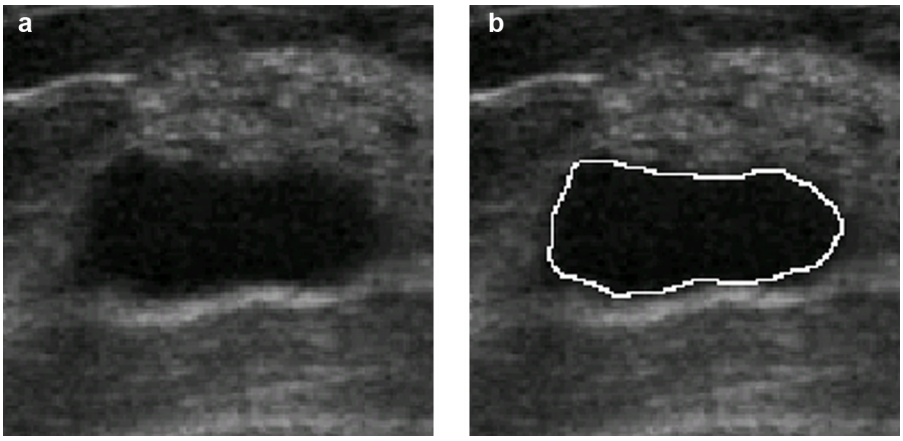

Fig. 6 – An example of a malignant tumor that was classified correctly by the proposed CAD algorithm but misclassified by the conventional CAD method. Among six predicted BI-RADS findings of this tumor, there were five benign findings: oval, parallel, microlobulated, abrupt interface, and no posterior acoustic features. Hypoechoicity was the only malignant finding that made this tumor to be classified as malignant in the diagnostic algorithm. The malignancy score of this tumor is 0.5 in the diagnostic algorithm. (a) The original sonographic image and (b) the contour outlined for feature extraction.

methods used by breast radiologists in clinical practice, Any tumor with one or more malignant findings was classified as malignant and only the tumors that had no malignant findings and at least one benign finding were classified as benign. The performance of our CAD system was as good as that of the radiologist (sensitivity: 100% vs. 99.8%, specificity: 37% vs. 30.5%) in Stavros' study [20]. There were some limitations of this study. First, the pool of malignant tumors collected for this experiment was not sufficiently diverse. Most malignant cases were invasive ductal carcinomas. To verify the applicability of the proposed CAD system, more types of malignant tumors, such as invasive lobular carcinoma and ductal carcinoma in situ, should be included in further investigation. Meanwhile, more quantitative features will be proposed to describe characteristics of various tumor types. Second, only two experienced radiologists from a single academic institution were involved in the assessment of the sonographic characteristics of breast tumors. Even though the BI-RADS lexicon has been confirmed to be appropriate for reducing interobserver variability [2], the consistency of the assessments of the different radiologists makes the result more convincing. Third, we did not perform reader study in this study. The results will be interesting whether our CAD system can improve radiologists' performance in the classification of breast tumors. For the generalization ability of the proposed CAD system to new cases, another limitation was the use of all tumors in feature selection before any further classification. The feature information was obtained from all tumors and was used in the validation of the experiment. With the extension of the US database in the future study, both AUC and pAUC of the proposed method will also be analyzed if they are significantly better than those of the conventional method.

Conflict of interest statement

The authors or authors' institutions have no conflict of interest.

Acknowledgements

The authors thank the National Science Council (NSC 99-2221-E-002-136-MY3), Ministry of Economic Affairs (100-EC-17-A-19-S1-164), and Ministry of Education (AE-00-00-06) of the Republic of China for the financial support. This study was also supported by a grant from the Innovative Research Institute for Cell Therapy and the Korea Healthcare Technology R&D Project, Ministry for Health, Welfare & Family Affairs.

REFERENCES

[1] American College of Radiology, Breast Imaging Reporting and Data System, 4th ed., American College of Radiology, Reston, VA, 2003.
[2] E. Lazarus, M.B. Mainiero, B. Schepps, S.L. Koelliker, L.S. Livingston, BI-RADS lexicon for US and mammography: interobserver variability and positive predictive value, Radiology 239 (2006) 385–391.
[3] D.R. Chen, R.F. Chang, W.J. Kuo, M.C. Chen, Y.L. Huang, Diagnosis of breast tumors with sonographic texture analysis using wavelet transform and neural networks, Ultrasound in Medicine and Biology 28 (2002) 1301–1310.
[4] W.J. Kuo, R.F. Chang, W.K. Moon, C.C. Lee, D.R. Chen, Computer-aided diagnosis of breast tumors with different US systems, Academic Radiology 9 (2002) 793–799.
[5] R. Malladi, J.A. Sethian, B.C. Vemuri, Shape modeling with front propagation—a level set approach, IEEE Transactions on Pattern Analysis and Machine Intelligence 17 (1995) 158–175.
[6] J.S. Suri, Advances in Diagnostic and Therapeutic Ultrasound Imaging, Artech House, Boston, London, 2008.
[7] R. Deriche, Fast algorithms for low-level vision, IEEE Transactions on Pattern Analysis and Machine Intelligence 12 (1990) 78–87.
[8] R.M. Rangayyan, N.R. Mudigonda, J.E.L. Desautels, Boundary modelling and shape analysis methods for classification of mammographic masses, Medical and Biological Engineering and Computing 38 (2000) 487–496.

[9] K. Nie, J.H. Chen, H.J. Yu, Y. Chu, O. Nalcioglu, M.Y. Su, Quantitative analysis of lesion morphology and texture features for diagnostic prediction in breast MRI, Academic Radiology 15 (2008) 1513–1525.
[10] R.M. Haralick, ShanmugaK., I. Dinstein, Textural features for image classification, IEEE Transactions on Systems, Man and Cybernetics Smc3 (1973) 610–621.
[11] W.C. Shen, R.F. Chang, W.K. Moon, Y.H. Chou, C.S. Huang, Breast ultrasound computer-aided diagnosis using BI-RADS features, Academic Radiology 14 (2007) 928–939.
[12] D.W. Hosmer, Applied Logistic Regression, 2nd ed., Wiley, New York, 2000.
[13] W.C. Shen, R.F. Chang, W.K. Moon, Computer aided classification system for breast ultrasound based on breast imaging reporting and data system (BI-RADS), Ultrasound in Medicine and Biology 33 (2007) 1688–1698.
[14] E. Alpaydin, Introduction to Machine Learning, MIT Press, Cambridge, MA, 2004.
[15] A.P. Field, Discovering Statistics Using SPSS, 3rd ed., Sage Publications, Los Angeles, 2009.
[16] X. Robin, N. Turck, A. Hainard, N. Tiberti, F. Lisacek, J.C. Sanchez, M. Muller, pROC: an open-source package for R and S plus to analyze and compare ROC curves, BMC Bioinformatics 12 (2011).
[17] N. Cho, W.K. Moon, J.M. Chang, A. Yi, H.R. Koo, B.K. Han, Sonographic characteristics of breast cancers detected by supplemental screening US: comparison with breast cancers seen on screening mammography, Acta Radiologica 51 (2010) 969–976.
[18] M.S. Bae, W. Han, H.R. Koo, N. Cho, J.M. Chang, A. Yi, I.A. Park, D.Y. Noh, W.S. Choi, W.K. Moon, Characteristics of breast cancers detected by ultrasound screening in women with negative mammograms, Cancer Science 102 (2011) 1862–1867.
[19] S. Joo, Y.S. Yang, W.K. Moon, H.C. Kim, Computer-aided diagnosis of solid breast nodules: use of an artificial neural network based on multiple sonographic features, IEEE Transactions on Medical Imaging 23 (2004) 1292–1300.
[20] A.T. Stavros, Breast Ultrasound, Lippincott Williams & Wilkins, Philadelphia, PA, 2004.
[21] J.L. Jesneck, J.Y. Lo, J.A. Baker, Breast mass lesions: computer-aided diagnosis models with mammographic and sonographic descriptors, Radiology 244 (2007) 390–398.
[22] S. Gefen, O.J. Tretiak, C.W. Piccoli, K.D. Donohue, A.P. Petropulu, P.M. Shankar, V.A. Dumane, L.X. Huang, M.A. Kutay, V. Genis, F. Forsberg, J.M. Reid, B.B. Goldberg, ROC analysis of ultrasound tissue characterization classifiers for breast cancer diagnosis, IEEE Transactions on Medical Imaging 22 (2003) 170–177.